

On the Resolution Transfer Sequence that Results in Monotonic Changes of Area-Averaged Two-Band Spectral Vegetation Indices

Kenta Obata^a, Hiroki Yoshioka^{b*}

Department of Information Science and Technology, Aichi Prefectural University, 1522-3 Kumabari, Nagakute, Aichi, Japan.

^a kenta.obata@cis.aichi-pu.ac.jp ^b yoshioka@ist.aichi-pu.ac.jp

Abstract – Spectral vegetation indices (VI) using two spectral bands (two-band VI) have been widely used to monitor vegetation status for the last four decades. In those VIs, systematic biases have been observed due to differences in spatial resolution, known as scaling effect. To understand its mechanism and then predict error bounds caused by the scaling effect, monotonic behavior of spatially averaged VI along with resolution changes has been discussed by several researchers. This study introduces theoretical framework regarding resolution transfer sequence in which area-averaged two-band VI surely varies monotonically. The definition of such a resolution sequence, called resolution class, is explained thoroughly. A set of numerical experiments have been conducted to validate the monotonic behavior of VIs. From the result the validity of the proposing framework has been confirmed.

Keywords: scaling effect, resolution class, two-band vegetation indices, linear mixture model, monotonic behavior

1. INTRODUCTION

Global Earth Observation System of Systems (GEOSS) is operated by GEO works for long-termed and consistent monitoring of earth surface environment, and provides an important scientific basis and decision making in every sector of our society including climate, energy, agriculture, biodiversity and numerous other areas (Lautenbacher, 2005). In the system, multiple data sources of earth observation based on satellite or airplane remote sensing as well as ground measurements have been integrated to achieve its goal. In this context, Land surface imaging (LSI) constellation system plays an important role for land surface monitoring in which four decades of satellite images from various optical sensors of middle resolution (10~100m) are archived (Bailey, 2007). To facilitate environmental monitoring with high accuracy, integration of the data of different sensors from calibration point of view is considered as indispensable efforts/tasks (Tucker, 2005).

However, in general, data from multiple sensors tend to be suffered from biases due to differences in sensor characteristics such as spatial and spectral resolution (Brown, 2006). Hence, the

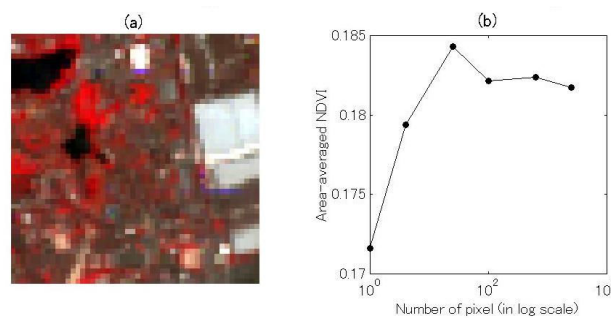


Figure 1. Transition of NDVI as a function of spatial resolution. (a) False color image on target field observed by Landsat7/ETM+ for sub-urban area. (b) Area-averaged NDVI as a function of spatial resolution (number of pixel).

problems caused by the sensor differences need to be overcome.

Spatially averaged values of spectral vegetation indices (VIs) using red and near infrared (NIR) bands, e.g. NDVI, SAVI and EVI2, shows some degree of dependencies on spatial resolution (Obata, 2011). The systematic errors in two-band VI induced by differences in spatial resolution are known as scaling effect (Aman, 1992; Cola, 1997; Maselli, 1998; Jiang, 2006). Especially the scaling effect of NDVI has been investigated intensively from empirical viewpoints (Thenkabail, 2004), numerical simulations (Huete, 2005), and analytical approaches (Hu, 1997). One example of the scaling effect in area-averaged NDVI is introduced in Fig. 1. The false color image on the target field is shown in Fig.1 (a). Figure (b) is a plot of the area-averaged NDVI as a function of spatial resolution (the number of pixels). Several studies have discussed the trend of NDVI (Hu, 1997; Jiang, 2006) by mentioning its monotonic behavior under a certain condition where the land surface is composed of two components (vegetated and non-vegetated surface). Monotonicity turns out to be an important aspect from calibration point of view. If we are able to identify the factor that determines the monotonic behavior and their trend (increasing or decreasing), the bias prediction would be easier.

Yoshioka et al. has introduced a condition under which the averaged NDVI changes monotonically along with spatial resolution (Yoshioka, 2008). Although their study shows the existence of the resolution sequence along which the NDVI value changes monotonically, thorough discussion about the framework of the theory remains undone. The accompany paper (Obata, 2011) discussed a proof of monotonic behavior subjecting two-band VI in general form by expanding the theory on NDVI

* Corresponding author

** This work was supported by the Circle for the Promotion of Science and Engineering (KO), and JSPS KAKENHI 21510019 (HY).

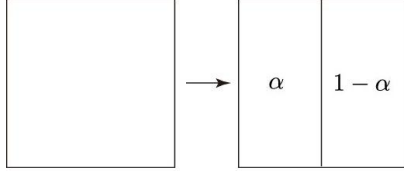


Figure 2. Illustration of resolution transfer from level 1 in to 2.

scaling effect. The objective of this study is to discuss a framework of the theory, specifically about the condition on the resolution sequence.

2. BACKGROUND

To model a series of resolution transition, a simple partitioning rule has been proposed (Yoshioka, 2008) as illustrated in Fig. 2. The number of pixels within a target area represents spatial resolution, expressed as ‘resolution level’ in this study. The resolution transfer is modeled by applying the partitioning rule (Fig. 2) to one of the pixels. In Fig. 2, the variable α represents a proportional area after the partitioning process. Then one resolution level will be transferred to the next level by applying this partitioning rule only once. Any resolution case will be reached from the original 1x1 case (the coarsest level) by repeating this process for a number of times necessary to achieve the designated resolution level. Variations of the VI value can also be modeled by averaging the VI values over the region.

Under the two-endmember assumption, magnitude relationship of spatially averaged two-band VIs between i -th and $(i+1)$ -th level (v_i and v_{i+1}) was investigated analytically (Obata, 2011) as

$$v_{i+1} \begin{cases} \geq v_i, & \text{if } \eta_k < 1, \\ = v_i, & \text{if } \eta_k = 1, \\ \leq v_i, & \text{if } \eta_k > 1, \end{cases} \quad (1)$$

with the definition of

$$\eta_k = \frac{\rho_{V,N} + k\rho_{V,R}}{\rho_{S,N} + k\rho_{S,R}} \quad (2)$$

where $\rho_{V,R}$ and $\rho_{V,N}$ are red and near infrared (NIR) reflectance of vegetation endmember spectrum, and $\rho_{S,R}$ and $\rho_{S,N}$ are red and NIR reflectance of non-vegetation endmember spectrum in the coordinate system of transformed space (Obata,

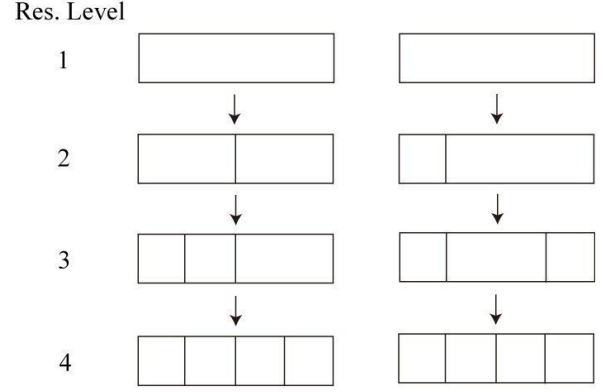


Figure 3. Examples of resolution classes from resolution level 1 to 4.

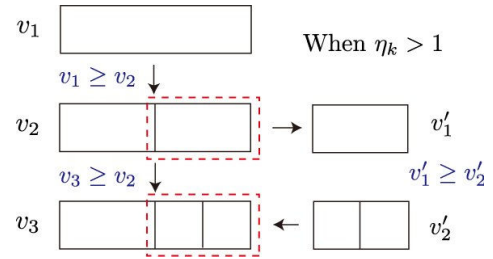


Figure 4. Illustration about monotonicity of spatially averaged two-band VI within a resolution class.

2011). The coefficient k depends on a choice of two-band VI. For example, in the case of NDVI and SAVI, k becomes 1, while k is 2.4 for EVI2. If η_k is smaller than 1, v_{i+1} is equal or larger than v_i . On contrary, if η_k is larger than 1, v_{i+1} is equal or smaller than v_i . Finally, the scaling effect never arises when η_k is equal to 1.

3. RESOLUTION CLASS

In order to proceed our discussion, we will define a sequence of resolution cases, ‘resolution class,’ in this section. A resolution transfer sequence generated by the repetition of the partitioning rule is defined as ‘resolution class.’ Two examples of resolution class with one-dimensional array are illustrated in Fig. 3. Note that although we use one-dimensional case as an example, this concept can be easily extended to the ordinal two-dimensional case (imageries).

Monotonic behavior of VI in a resolution class (along with spatial resolution) can be proved by the following analogy. From Eq. (1) area-averaged two-band VI after a single partitioning process (v_2) will be smaller than the value before the partitioning (v_1) when η_k is larger than 1 as illustrated in Fig. 4. Under this condition, averaged value of two-band VI within a resolution

class decreases monotonically from coarser to finer resolution (Fig. 4). Back to the explanation of Fig. 3, each sequence in Fig. 3 results in monotonic behavior based on the above analogy. On contrary, since these two sequences belong to different resolution classes, mixture of these two sequences may not show monotonic behavior. (Although it may happen to be monotonic, monotonicity is not guaranteed.)

4. NUMERICAL SIMULATION

The monotonic behavior of spatially averaged two-band VI within a resolution class will be validated by numerical simulations. We assumed one-dimensional array with the same size of nine pixels as a target field illustrated in Figs. 5(a) and 6(a). The sample consists of only two types of surfaces (vegetation and non-vegetation). To vary the trend (increasing or decreasing), two sets of endmember spectra have been assumed; one (EM1) results in $\eta_k > 1$ by setting spectra of (0.05, 0.35) and (0.1, 0.1) in red-NIR reflectance subspace for vegetation and non-vegetation, respectively. The other (EM2) results in $\eta_k < 1$ by setting (0.05, 0.35) and (0.3, 0.3) for vegetation and non-vegetation, respectively.

Reflectance spectra of nine levels of spatial resolution (level 1 to 9) were prepared to simulate reflectance spectra at various resolutions by averaging endmember spectra for each field. A reflectance spectrum at resolution level 1 is an area-averaged spectrum over the entire target field, and spectral data set of i -th resolution level is generated by setting $i-1$ boundaries and by performing spatial averaging for each pixel determined by the boundaries. The partitioning process is applied eight times to yield 9-th resolution level. As a result, there are $8! = 40320$ ways to generate the resolution transfer sequences, meaning that 40320 resolution classes were simulated in the simulation. Based on our theory, we expect that the area-averaged two-band VI varies monotonically for all the 40320 classes.

5. RESULTS

Figure 5 shows the variations of area-averaged NDVI, SAVI, and EVI2 as a function of spatial resolution for the case of EM1 in which the value of η_k is greater than 1. Figures 5 (b-d) show the VI variations for all the 40320 classes. We confirmed that all the cases show the decreasing trend as predicted from the theory, which indicates validity of our theory. Differences among VI can be seen as differences in magnitude of the error bounds.

Figure 6 shows the same plots as Fig. 5 for different endmember spectra (EM2). In this case, we expect increasing trend based on the theory, which can be confirmed in Figs. 6 (a-d).

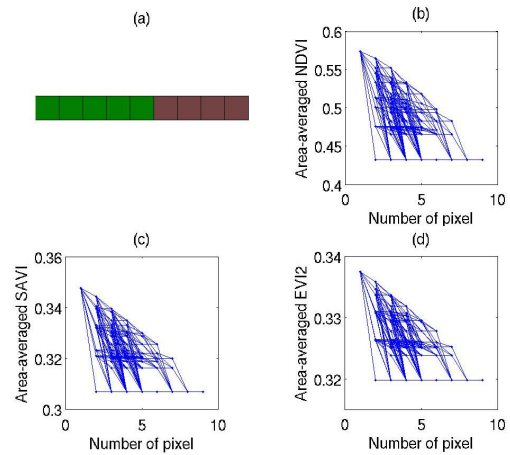


Figure 5. Monotonic behavior of spatially averaged two-band VI along with the number of pixels for EM1. (a) The target field consists of vegetation and dark soil. (b-d) show area-averaged two-band VI as a function of spatial resolution for 40320 resolution classes.

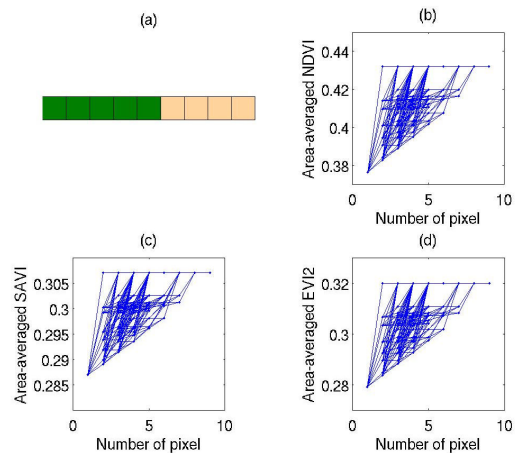


Figure 6. Monotonic behavior of spatially averaged two-band VI along with the number of pixels for EM2. (a) The target field consists of vegetation and bright soil. (b-d) show area-averaged two-band VI as a function of spatial resolution for 40320 resolution classes.

Figure 7 shows the results of EM1 case with different distribution of two endmembers to see the influence of heterogeneity. From the results, the trend (decreasing) stays the same as Fig. 5, which confirms the fact that the heterogeneity does not affect its trend (as was predicted from the theory). Note that the difference from Fig. 5 is the fact that the averaged VI values does not approach to the asymptotic value at early stage of resolution level. The reason is that pixel cannot be homogeneous at early level of resolution due to its heterogeneity comparing to Fig. 5.

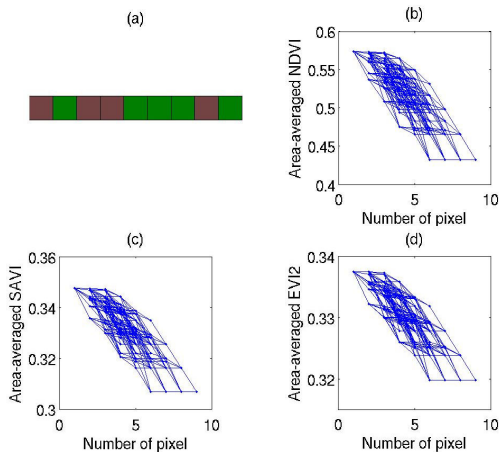


Figure 7. Monotonic behavior of spatially averaged two-band VI along with the number of pixels with different heterogeneity from Fig. 5.

6. DISCUSSION

This study introduced a framework for analysis of the scaling effect in two-band VIs expressed by a general form of model equation. The analysis becomes easier by knowing the fact that there are certain sequence of resolutions along which spatially averaged VI shows monotonic behavior. The resolution sequence was defined as ‘resolution class’, which is generated by applying simple partitioning processes repeatedly. We also introduced a key parameter to identify its trend (either increasing or decreasing) which can be written as a function of endmember spectra.

Numerical simulations have been conducted to examine validity of our theory. It was successfully demonstrated that the trend predicted from the theoretical analysis indeed explains the results obtained from the experiments.

Knowing the fact that averaged VI value changes monotonically under a certain condition, we take a step forward in predicting error bounds of VI value caused by resolution differences. It would also contribute to inter-sensor calibration on spatial resolution for various data products including fraction of vegetation cover and LAI.

REFERENCES

A. Aman, H. P. Randriamanantena, A. Podaire, F. Frouin, “Upscale integration of normalized difference vegetation index: the problem of spatial heterogeneity”, *IEEE Trans. Geosci. Remote Sens.*, vol. 30, p.p. 326-338, 1992.

G. B. Bailey, M. Berger, H. Jeanjean, “The CEOS Constellation for Land Surface Imaging”, in *Proc. SPIE*, vol. 6744, 674425, 2007.

M. E. Brown, J. E. Pinzon, K. Dian, J. T. Morisette, C. J. Tucker, “Evaluation of the consistency of long-term NDVI time series derived from AVHRR, SPOT-vegetation, SeaWiFS, MODIS, and Landsat ETM+ sensors”, *IEEE Trans. Geosci. Remote Sens.*, vol. 44, p.p. 1787-1793, 2006.

L. D. Cola, “Multiresolution covariation among Landsat and AVHRR vegetation indices”, in *Scale in Remote Sensing and GIS*, D. A. Quattrochi and M. F. Goodchild, Eds. Boca Raton, Florida: Lewis, p.p. 73-91, 1997.

Z. Hu, S. Islam, “A frame work for analyzing and designing scale invariant remote sensing algorithms”, *IEEE Trans. Geosci. Remote Sens.*, vol. 35, p.p. 747-755, 1997.

A. R. Huete, H.-J. Kim, T. Miura, “Scaling dependencies and uncertainties in vegetation index - biophysical retrievals in heterogeneous environments”, in *Proc. IEEE IGARSS05*, vol. 7, p.p. 5029-5032, 2005.

Z. Jiang, A. R. Huete, J. Chen, Y. Chen, G. Yan, X. Zhang, “Analysis of NDVI and scaled difference vegetation index retrievals of vegetation fraction”, *Remote Sens. Environ.*, vol. 101, p.p. 366-378, 2006.

C. C. Lautenbacher, “The global earth observation system of systems (GEOS),” in *Proc. International Symposium on Mass Storage Systems and Technology*, p.p. 47-50, 2005.

F. Maselli, M. A. Gilbert, C. Conese, “Integration of high and low resolution NDVI data for monitoring vegetation in Mediterranean environments”, *Remote Sens. Environ.*, vol. 63, p.p. 208-218, 1998.

K. Obata, H. Yoshioka, “Monotonicity of two-band spectral vegetation index in general form under a two-endmember linear mixture model”, in *Proc. 34-th International Symposium on Remote Sensing of Environment*, 2011.

P. S. Thenkabail, “Inter-sensor relationships between IKONOS and Landsat-7 ETM+ NDVI data in three ecoregions of Africa,” *Int. J. Remote Sens.*, vol. 20, p.p. 389-408, 2004.

C. J. Tucker, J. E. Pinzon, M. E. Brown, D. A. Slayback, E. W. Pak, R. Mahoney, E. F. Vermonte, N. E. Saleous, “An extended AVHRR 8-km NDVI dataset compatible with MODIS and SPOT vegetation NDVI data,” *Int. J. Remote Sens.*, vol. 26, p.p. 4485-4498, 2005.

H. Yoshioka, T. Wada, K. Obata, T. Miura, “Monotonicity of area-averaged NDVI as a function of spatial resolution based on a variable endmember linear mixture model,” in *Proc. IGARSS2008*, vol. 3, p.p. 415-418, 2008.